SHORT REVIEW

CROATICA CHEMICA ACTA

Croat. Chem. Acta **2020**, *93*(1), 1–14
Published online: October 20, 2020
DOI: 10.5562/cca3640

HKD 1926

Determination of Au Film Thiolation and Silane Bonding Onto SiO_2 Films Within the Frame of Biosensor Surface Functionalization – an Analysis of Best Practices and Techniques

Leda G. Bousiakou,[1,2,*] Stefanos Karapetis[3]

[1] IMD Laboratories Co, R&D Section, Lefkippos Technology Park, NCSR Demokritos PO Box 60037, GR-15130 Agia Paraskeyi, Athens, Greece
[2] Department of General Sciences (DGS), Prince Sultan University, PO BOX 66833, Riyadh 11586, Saudi Arabia
[3] Laboratory of Inorganic & Analytical Chemistry, School of Chemical Engineering, Dept of Chemical Sciences, National Technical University of Athens, 9 Iroon Polytechniou St., GR 15780, Athens, Greece
* Corresponding author's e-mail address: leda@imdlaboratories.gr

RECEIVED: April 22, 2020 * REVISED: August 31, 2020 * ACCEPTED: September 13, 2020

Abstract: This paper reviews some of the most common surface modification approaches in biosensing based on self-assembled monolayers with a particular focus on Au film thiolation and SiO_2 film silanization. Such approaches are routinely used to alter the materials' surface properties towards a desired bioresponse. Furthermore, the most appropriate characterization methods towards ensuring successful surface modification are presented including XPS, HREELS, SPFS, Raman and FTIR spectroscopy as well as UPS with specific examples to demonstrate their importance. In addition, the mechanisms of fluorescent and non-fluorescent biotinylation of thiolated Au films and silanized SiO_2 are discussed considering its importance in conjugating biomolecules such as enzymes, antibodies or chemokines onto surfaces, which carries high significance for biosensing applications. Finally, within this frame characterization routes towards ensuring effective attachment are discussed.

Keywords: biosensing, SAMs, Au, thiolation, silanes, silanization, characterization, biotinylation, fluorescence.

INTRODUCTION

THERE has been extensive research in the area of self-assembled monolayers (SAMs) within the frame of biosensor surface functionalization.[1–3] SAMs are two-dimensional nanomaterials that form spontaneously on a variety of solid surfaces in a highly ordered fashion, through the process of self-assembly of their molecular components.[4–7] In particular SAM formation is one of the simplest approaches in achieving thermodynamically stable monolayers through strong chemisorption that is in contrast to Langmuir-Blodgett and other techniques that lead to physisorption and unstable mono or multilayer films.[8] Specifically, in SAMs the adsorption of a surfactant with a specific affinity leads to the chemisorption of *head* groups onto a substrate from either the vapor or liquid phase, followed by the slow organization of *tail* groups. In particular, at low molecular densities, the adsorbed molecules result in a more disordered phase, while as the density increases molecules can form a 2-dimensional phase.[9,10] Over longer timescales, from minutes to hours, semicrystalline or 3-dimensional crystalline structures can form.[11] The simplest approach for the formation of such unimolecular organic films is via immersion of e.g. a noble metal surface in a dilute solution of the organic molecule at ambient conditions. In general, SAM formation is one of the simplest and most effective routes towards achieving organic films, utilizing both aliphatic and aromatic molecules that contain functional groups such as SH, –CN, –COOH, $–NH_2$ as well as silanes on selected metallic (Au, Cu, Ag, Pd, Pt, Hg, and C) or semiconducting surfaces (Si, GaAs, ITO, etc).[12]

In particular, organic SAMs are widely used in biosensor fabrication due to their flexibility of design and potential to combine organic and biological molecules.

SAMs are indeed a powerful and flexible approach in immobilizing proteins, enzymes, DNA etc on solid surfaces providing one of the most suitable functional interlayers.[13] Currently some of the most widely used SAMs in biosensing are thiols on Au surfaces and alkylsilanes on oxides, due to their relatively straightforward preparation leading to densely packed monolayers.[16] Generally, both types of thiols (R–SH or –C–SH)[14,15] and silanes ($R\text{-}Si(OH)_3$) are strong surface anchors leading to chemisorption with the former binding well to metals, such as Au, Ag, Pt and Cu, while the latter binding preferably to surfaces such as SiO_2, indium tin oxide (ITO) and TiO_2. It is noted that within molecular immobilization chemisorption does not necessarily entail the presence of a full covalent bond, but also refers to charge-transfer (CT) complexes. In general, surface functionalization requires the creation of an appropriate surface chemistry using a number of different molecular components in specific order. Within this frame *surface anchors* provide stable binding to the substrate material while spacers screen all interactions between target and substrate. Finally, a functional unit, otherwise called the recognition element is used to selectively capture the target (Figure 1a). We note that nanoscale biosensors can consist of more than one, i.e. two different substrate materials and thus require variations in the functionalization process (Figure 1b).

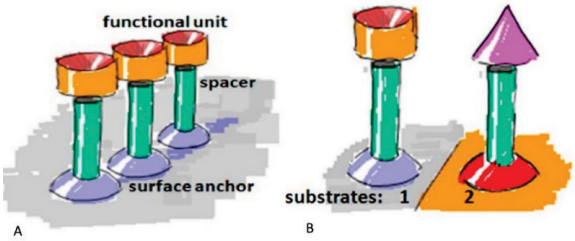

Figure 1. (a) The different molecular components required to create a biosensor surface: anchor, spacer and functional unit (b) working with more than one substrate material.[16]

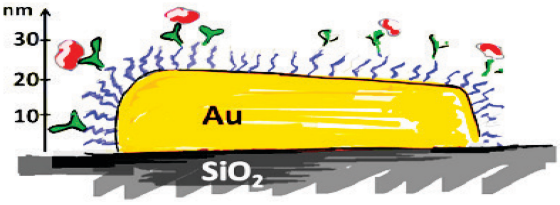

Figure 2. A thin film of Au (nm scale) supported on a SiO_2 substrate.[16]

In the case of thiols on Au-substrates, we have the irreversible binding of the thiol group to the Au surface whose thickness is in the nm scale (Figure 2).

Thiols are organosulfur compounds expressed with the general chemical formula (–C–SH or R–SH). In general, a *sulfhydryl or thiol group* (–SH) is bonded to carbon containing atoms, such as alkanes which are represented as R. During thiolation clean metal surfaces such as Au are immersed for 12–18 h in dilute ethanolic solutions of thiols (1–10 mM at room temperature) in order to prepare SAMs.[17] In order to minimize defects in SAM formation and maximize the layer density, a slow reorganization process of hours is recommended. In general, there is a preference to Au substrates as they form good quality SAMs, and also Au does not react with atmospheric O_2 being an inert metal. Once thiol molecules react with an Au film an interface of approximately 2 nm thickness is formed. In Figure 3, a simple alkanethiol molecule is depicted as it attaches to the Au surface. The anchoring on the Au substrate is achieved by the sulfur binding group, while the C12 alkanethiol chain, i.e. the spacer, consists of the methylene groups ($–CH_2–$). The head group or otherwise the functional group, allows to target the desired molecules selectively producing the desired surface chemistry.

Moreover, sulfur containing polymers have also been reported to adsorb directly to a gold surface. In particular according to Tam-Chang et al.,[20] poly(3-octylthiophene)

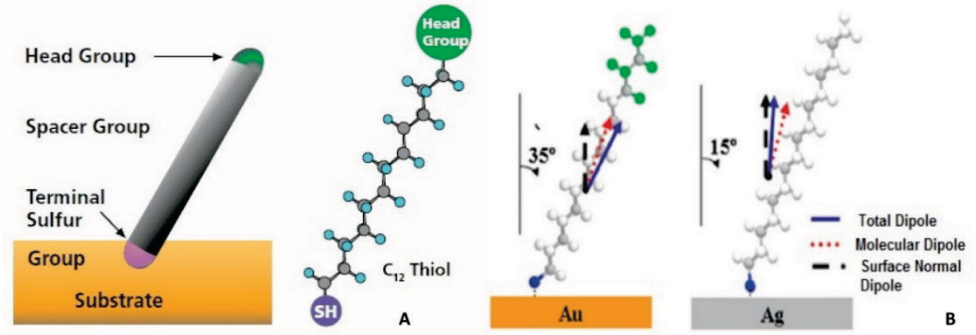

Figure 3. (A) The linking of the sulfur group to the Au substrate with the functional (head) group allowing for the desired surface chemistry[18] (B) Achieving different bond angles/directions for thiols on a gold and silver substrates.[19]

(POT) can form a stable self-assembled film on Au electrodes. Furthermore, the insulating POT layer can be converted to a conducting film upon doping with chemical oxidants such as iodine.

We note that surface gradients in SAMs (Figure 4) allow for physiochemical property variations that can evolve in time and provide a mechanism for further modulation of the interfacial properties. In general, such surface gradient manipulation allows for the presence of a wide range of properties in single specimens leading to the simultaneous analysis of several parameters without the need of using numerous samples.[6]

In the case of silanization ($R–Si(OH)_3$) of silicon dioxide (SiO_2) film substrates, silanes are utilized. In particular, silane molecules[21,22] contain silicon (Si) at the center of the molecule which attaches to two functional groups, denoted as (R) and (X) (Figure 5). In this case (R) represents an organic functional group (e.g. vinyl, amino, chloro, etc.) which attaches to organic resins, while (X) can hydrolyze producing silanol, leading to siloxane or metal oxide bonds with inorganic substrates.

Silanization of biosensor surfaces (Figure 6) usually involves the covalent attachment of primary amines such as APTES (3-aminopropyl trimethoxy silane) to silica thin films using coupling agents (di-alkoxy silanes, mono-alkoxy silanes, tri-alkoxy, etc.). The most preferable inorganic substrate in this case is SiO_2, because it is versatile and chemically stable.[23,24]

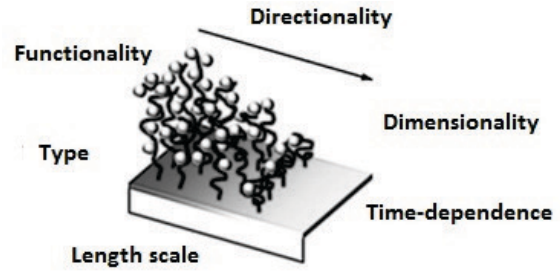

Figure 4. Surface chemical gradient characteristics.[6]

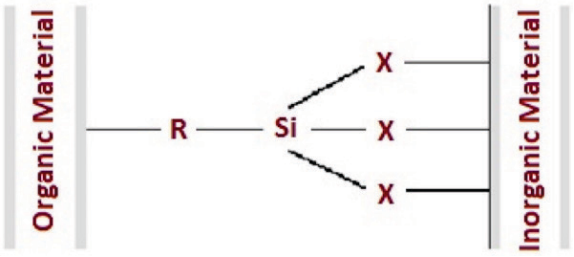

Figure 5. Silane attachment to organic and inorganic substrates.[22]

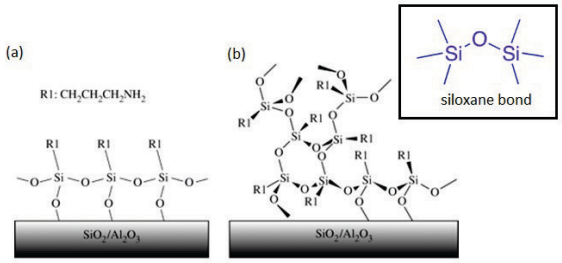

Figure 6. Schematics representation of a silane films (SAMs) on a SiO_2 / Al_2O_3 substrate using an (a) idealized APTES and (b) multilayered APTES.[25]

CHARACTERIZATION PROCESSES: DETERMINING THE PRESENCE OF THIOLS (R–SH OR –C–SH) ON Au SUBSTRATES

In general, both spectroscopic and microscopic techniques are commonly employed in order to characterize the SAMs on solid surfaces. Raman spectroscopy is a chemical fingerprinting technique that can determine the presence of thiols on Au surfaces, in form of vibrational spectra, with little sample preparation and at a low cost. In particular surface enhanced Raman spectroscopy (SERS) can provide an enhanced signal (10^4–10^6 orders) due to surface plasmon contributions especially on noble metal surfaces such as Au, Ag and Pd whose roughness is in the nm scale.[26–29] Additionally, a number of other characterization techniques[17] such as X-ray photoelectron spectroscopy (XPS), high resolution electron energy loss spectroscopy (HREELS) and time of flight secondary ion mass spectrometry (ToF-SIMS)[30] have also been used to provide chemical state analysis of thiolated Au surfaces.[31]

Other approaches in SAM characterization include ellipsometry that measures SAM thickness, while order and orientation of molecules can be examined using Near Edge X-ray Absorption, Fine Structure (NEXAFS)[32] and Reflection Absorption Infrared Spectroscopy (RAIRS).[33,34] Furthermore, Scanning Tunneling Spectroscopy (STM) and atomic force spectroscopy (AFM) can be used to examine SAM structure.[35] In particular, STM can image the shape, spatial distribution, terminal groups and their packing structure. Moreover, even though AFM[36] is used primarily to measure sample topography, it has been also used by Langry et al.[37] in force calibration mode in order to measure the tensile stress of thiols bonded to Au surfaces.

An alternative characterization instrument for measuring the self-assembly in real time is dual-polarization interferometry (DPI) where the refractive index, thickness, mass and birefringence of the self-

assembled layer can be quantified at high resolution.[38,39] The kinetics of adsorption and temperature induced desorption as well as information on structure can also be obtained in real time by ion scattering techniques such as low energy ion scattering (LEIS) and time of flight direct recoil spectroscopy (ToF DRS).[40]

Surface Enhanced Raman Spectroscopy

Garrell et al.[41] demonstrate the use of SERS in investigating the interactions of aromatic thiols, i.e. Benzenethiol (BT) and benzenemethanethiol (BMT) on roughened Au electrode surfaces (Figure 7). The aim is to investigate further the behavior of thiols that are known to adsorb dissociatively on gold, i.e. with cleavage of the S–H bond. In particular, the Au electrode is initially immersed in an ethanol solution of the thiol, where the analyte concentration is 1 mM and then placed in 0.1 M KCl prior to the acquisition of the SER spectra.

The normal and surface enhanced Raman spectra of neat and aqueous benzenethiol are presented in Figure 8.

In the neat BT spectrum (–600mV) the bands at 617 cm^{-1} and 699 cm^{-1} are due to the C–S stretching vibration,

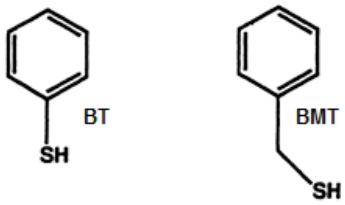

Figure 7. Benzenethiol (BT) and benzenemethanethiol (BMT).[41]

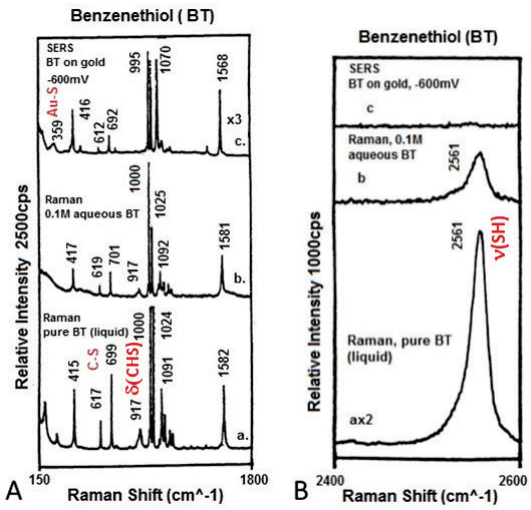

Figure 8. Normal and surface enhanced Raman spectra of neat (A) and aqueous (B) benzenethiol.[41]

while they both shift downward by about 8 cm^{-1} in the surface enhanced Raman spectrum. Additionally, the δ(CSH) and ν(SH) stretching vibrations which are present in the aqueous BT spectrum at 917 cm^{-1} and 2561 cm^{-1} disappear in the SER spectrum. These changes are evidence that BT adsorbs dissociatively from ethanol onto gold. Furthermore, the band at 359 cm^{-1} is due to the Au-S stretching vibration; it's frequency depends on the applied potential. In the case of BMT, the Au–S stretching vibration appears at 309 cm^{-1} in the –600mV spectrum (Figure 9).

In a full analysis of the Raman and SER spectra of BMT on Au[42] it is noted that the δ CSH and ν SH modes do not appear in the SER spectra as in the case of BT, suggesting again that BMT adsorbs dissociatively on gold through the sulfur atom. Furthermore, an intense spectrum in the C–H stretching region of the SER spectrum can provide further information on the orientation of the BMT attachment on the surface, i.e. suggesting that BMT attaches at an angle on the Au surface, rather than adsorbing almost flat as it does on Pt (111).[43] Moreover, any variations in the SER spectrum between +500 mV and –600mV are due to orientation changes in the BMT molecules that lead to stronger interactions between its rings and the Au surface. Any shift back to the –600mV potential does not received the original spectrum, which suggests changes in the surface coverage. Finally, BMT, like BT, desorbs at a potential between +800 and +1000 mV, and between –1000 and –1200 mV.

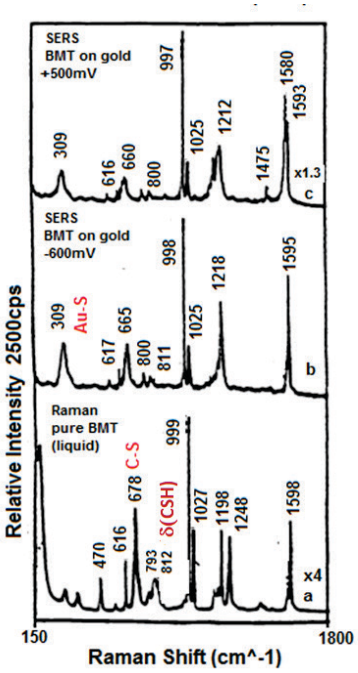

Figure 9. BMT normal and surface enhanced Raman spectra.[41]

X-ray Photoelectron Spectroscopy (XPS) and Ultraviolet Photoelectron Spectroscopy (UPS) Studies

Photoelectron spectroscopy allows for the study of surface elements, providing information about their chemical and electronic states. In particular, XPS, studies the emission of photoelectrons using soft-rays (200–2000) eV, while UPS[44] uses UV radiation (10–45) eV. In general, XPS can identify the characteristic binding energy, i.e. the work function of each surface element, at a depth of about 10 nm, giving rise to a set of peaks in the photoelectron spectrum. The intensity of these peaks can give an estimate of the element concentration in the sampled region. Additionally, depending on the operational mode, information can be inferred on the chemical bonding of the surface elements as well as their electron states.

Castner et al.[45] studied the adsorption of thiol and disulfide molecules on the surface of Au substrates, using XPS. Especially they monitored the $S_{2p3/2}$ binding energy (BE) to provide evidence on SAM formations, establishing that in the case of unbound thiol or disulfide species, the $S_{2p3/2}$ binding energy ranged from 163.5–164 eV, while upon binding, it decreased to 162 eV. Figure 10 shows the XPS spectra for C16–SH ($CH_3(CH_2)_{15}$–SH) and F8 thiol ($CF_3(CF_2)_7$–C(O)N(H)$(CH_2)_2$SH) adsorbed onto an Au surface, which are consistent with the above described observations. We note that the presence of unbound thiol molecules signifies that they are partially penetrated into

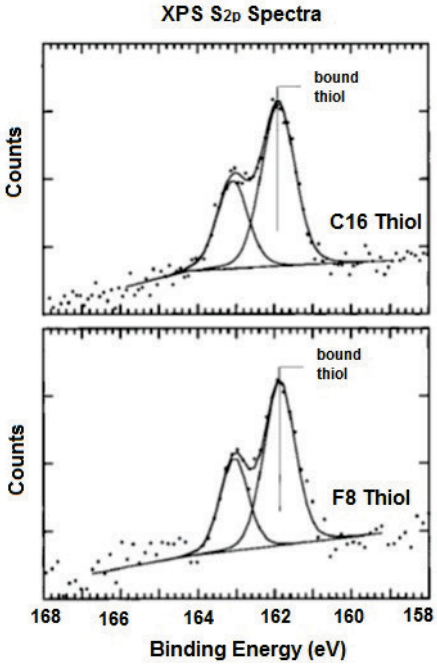

Figure 10. The XPS (S_{2p}) spectrum for C16SH (hexadecane thiol) and F8 thiol (perfluorooctyl-thiolate) adsorbed onto an Au surface.[45]

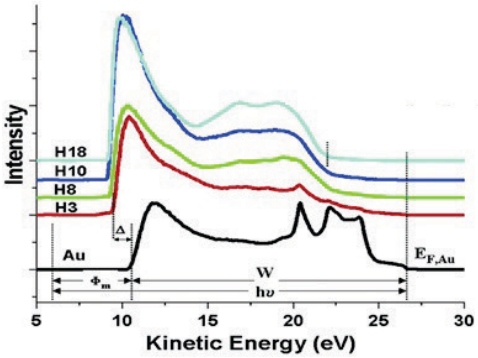

Figure 11. The UPS spectra for a clean gold surface and one modified using alkanethiols (H_3SH, H_8SH, $H_{10}SH$, and $H_{18}SH$).[46]

the self-assembled monolayer or they exist lying on top of it. Usually this occurs when poor solvents have been used for the preparation of thiol adsorption solutions, for instance use of ethanol for long chain alkanethiols. Additionally, unbound thiols can remain at the surface of a bound thiolate SAM when no rinsing has taken place.

UPS has been used to detect the presence of Au surface thiolation by studying the kinetic energy spectrum of the photoelectrons emitted by the molecules after UV irradiation. Alloway et al.[46] studied the UV photoemission spectra in the case of a clean Au surface. In this example an Au surface has been thiolated using the following alkanethiols: H_3SH, H_8SH, $H_{10}SH$, and $H_{18}SH$. Figure 11 shows the characteristic shift (Δ) in the kinetic energy.

High-resolution Electron Energy Loss Spectroscopy (HREELS)

Rousseau et al.[47] used high-resolution electron energy loss spectroscopy (HREELS), that is a sensitive surface science technique that looks at the energy losses of inelastically scattered electrons on the sample surfaces even at the MeV range, in order to study alkane thiolate SAMs on Au (111) surfaces. Particularly in this case the study was on the transformation of an initially weakly adsorbed dimethyl disulfide (DMDS) layer on Au (111) at T < 150 K into chemisorbed methylthiolate (MT) SAMs by heating at temperatures above 200 K.

The HREEL spectrum (Figure 12.) of the DMDS adsorbed layer at 100 K shows a large peak at 16 MeV associated to the Au–S stretching mode that is absent in the MT spectrum. The remaining bands at higher frequencies show a similarity to the MT layer without any further peaks present. At 250 K, we note that there is a red-shift of the Au–S stretching mode to 30 MeV. This red-shift of the Au–S stretching mode of the DMDS layer, relative to that of MT, indicates that the Au–S interaction in the former is weaker than in the latter.

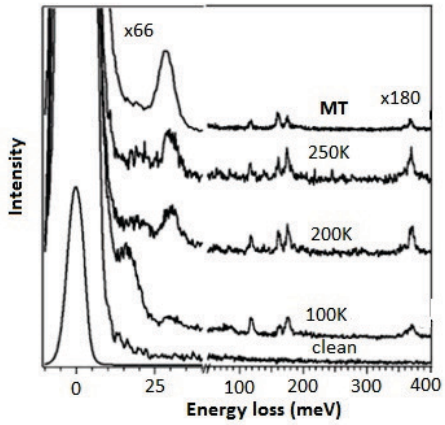

Figure 12. The HREEL spectrum of dimethyl disulfide at 100 K, 200 K and 250 K and methylthiolate.[47]

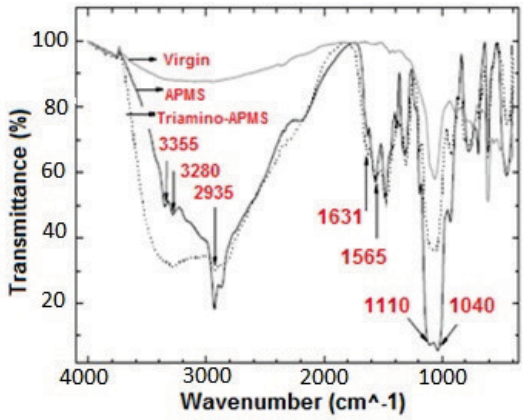

Figure 13. The normalized Fourier transform infrared spectrum after SiO_2 surface silanization with APMS and triamino APMS.[49]

CHARACTERIZATION PROCESS: DETERMINING THE PRESENCE OF SILANES ($R–Si(OH)_3$) ON SILICON DIOXIDE (SiO_2) SUBSTRATES

The silanisation of SiO_2 surfaces can be determined using a number of non-destructive surface science techniques as introduced previously, such as Raman spectroscopy, SERS and HREELS. Additionally, the use of Fourier transform infrared spectroscopy (FTIR) along with XPS can also provide valuable information on the surface chemistry of our samples, while AFM and STM can be utilized primarily for topological studies.

Fourier Transform Infrared Spectroscopy (FTIR)

Fourier Transform infrared spectroscopy, is a very useful chemical analysis technique, allowing us to obtain the infrared (IR) spectra, near to far IR, of a sample by collecting its interferogram and then performing its Fourier transform.[48]

Cherkouk et al.,[49] used FTIR to study the silanization procedure of SiO_2 surfaces using APMS (3-Aminopropyl trimethoxysilane) and tri-amino-APMS (N'-(3-trimethoxy-silyl)-propyl)-diethylenetriamine) coupling agents using a spray and spin coating method in a nitrogen atmosphere at room temperature for 10 min. As seen in Figure 13, a peak appears at 1060 cm^{-1} is due to the asymmetric stretching mode (Si–O–Si) from the silica substrate that shifted to 1040 cm^{-1} upon APMS film formation.

Additionally, the $Si–O–CH_3$ part of the propyl group of APMS and triamino-APMS lead to a second peak at 1110 cm^{-1} and at 1100 cm^{-1} respectively, as well as to further peaks at 2935 cm^{-1} and 2880 cm^{-1} belonging to the symmetric and asymmetric stretching mode. Furthermore, the free $R–NH_2$ on the silica surface gives rise at a signal at 1565 cm^{-1}, while at 1630 cm^{-1} there is a signal due to positively charged ammonia (NH_3^+). Thus the film deposition with APMS and triamino-APMS results in covalent binding of the methoxy part of the molecular structure to the surface.

Raman Scattering and X-ray Spectroscopy (XPS) Studies

The silanisation of the SiO_2 surface with AMPS has also been studied by Cherkouk et al.[49] using Raman spectroscopy (Figure 14) showing a presence of the valence stretching modes $\nu(NH_2)$ and $\nu(CHx)$ at 2810 cm^{-1} and 2890 cm^{-1} respectively. Furthermore, deformation bands of the $\delta(CH)$ mode appear at 1456 cm^{-1}, 1410 cm^{-1}, 1312 cm^{-1}, and at 1140 cm^{-1}. These features as argued by Cherkouk et al. reveal good coverage of the SiO_2 surface.

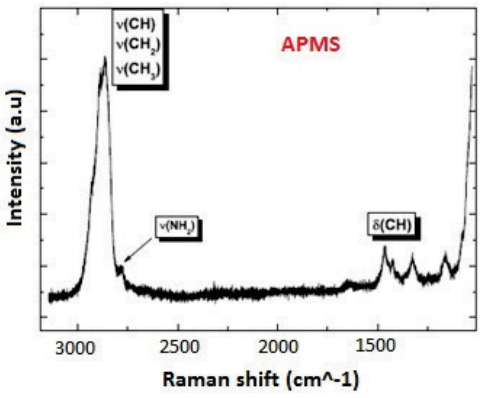

Figure 14. The Raman spectrum of the silica surface silanized with APMS.[49]

Similarly, XPS analysis[49] of the samples showed that when silanized by APMS or triamino-APMS using the spray and spin coating method, the Si^0 signals coming from SiO_2 significantly weaken compared with those from the untreated SiO_2, which is an indication of the surface coverage. Other XPS studies[50] on the modification of silica by 3-aminopropylethoxydimethylsilane (APTS) and 3-aminopropylethoxydimethylsilane (APREMS) showed that the polymerization of aminosilanes and consequently the thickness of the aminosilane layer depend on the number of possible bonding sites of the aminosilane molecule. In particular, the XPS spectra of the elements (Si, C, O and N) were identified and their concentrations calculated. In general, an increase in the C concentration and the appearance of an N peak in the XPS spectra show successful bonding of the aminosilane molecules to the surface.

Typical high-energy resolution N 1s and Si 2p spectra in this case are shown in Figures 15 and 16 below. In the N1s spectra two different components are identified related to NH bonds, i.e. the $–NH_2$ component which corresponds to a binding energy (BE) of 399.2 eV and the $–NH_3^+$ component which corresponds to BE = 401.0 eV. The ratio of the $–NH_2/–NH_3^+$ components provides us with information on the interactions present on the silicon substrate upon APTMS silanisation.

In the study of the Si 2p XPS spectrum four components are identified as can be seen in Figure 16.

The Si–Si bonds originating from the bulk silicon wafer beneath the oxide layer correspond to the 99.3 eV and 99.9 eV peaks. Additionally, the presence of the aminosilane on the SiO_2 surface corresponds to the 102.2 eV peak, while the 103.0 eV peak corresponds to the SiO_2 in the oxide layer.

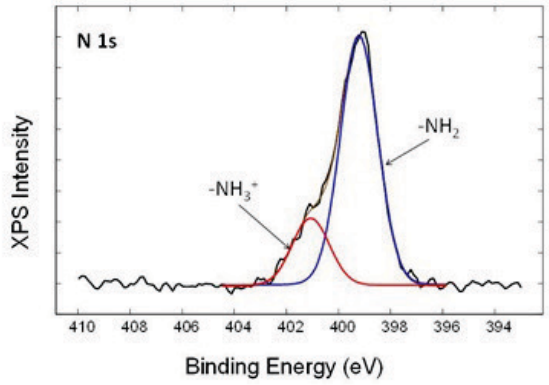

Figure 15. The (N 1s) XPS Spectra for the SiO_2 silanisation with APTMS.[50]

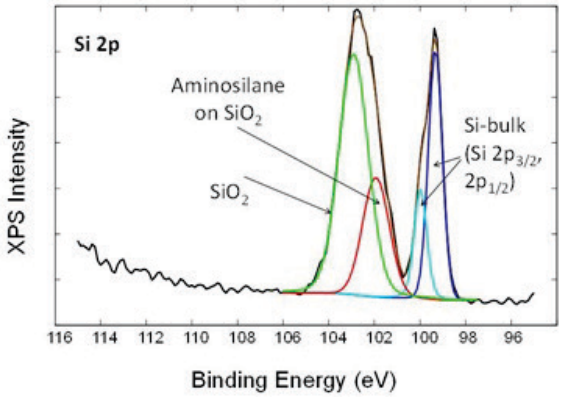

Figure 16. The (Si 2p) XPS Spectra for the SiO_2 silanisation with APTMS.[50]

FLUORESCENT AND NON-FLUORESCENT BIOTINYLATION OF THIOLATED Au SURFACES AND SILANIZED SILICON OXIDE FILMS

Biotin labelling is frequently used as a non-radioactive labelling of proteins and other target molecules, utilizing the stable, non-covalent interaction between biotin and either avidin, streptavidin or the neutravidin protein. Significant work within life science is currently devoted to the study of organic films containing biotin ligands that can allow for countless applications in fields such as affinity chromatography, immunoassays and biosensing.[51] In general, the biotin-(strept)avidin system is a widely used intermediate between the surface and the active biolayer. It is also employed as a model system to study biorecognition events between proteins and other biomolecules. Moreover, biomolecules such as proteins and DNA can be easily biotinylated and bound to (strept)avidin coated surfaces.

Within biosensing,[52] IR biosensors have been investigated with the functionalization of Au substrates with thin organic films containing biotin ligands, while in electrochemical biosensing the avidin-biotin system has been used for the fabrication of enzyme sensors in relation to the preparation of enzyme thin films in which enzymes are assembled into a layer-by-layer structure composed of monomolecular layers.

Earlier studies have shown that avidin binds to biotin, 8-oxodeoxyguanosine and related bases (Figure 17). These features of biotin and avidin are shared by streptavidin and the neutravidin protein. In particular, the binding of biotin to avidin is the strongest non-covalent interaction known with a dissociation constant $K_d \cong 10^{-15}$ M. Furthermore, avidin, streptavidin and the neutravidin protein, have the ability to bind up to four biotin molecules.

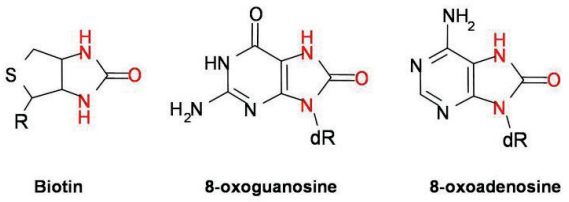

Figure 17. The biotin, 8-oxodeoxyguanosine and 8-oxodeoxyadenosine chemical structures.[53]

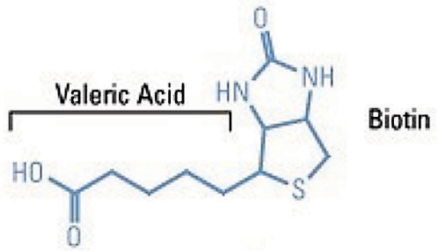

Figure 18. The valeric acid chain.[55]

In general, the key feature in the recognition of biotin is the *ureido functionality*[54] which is highlighted in Figure 17. The ureido group allows for the formation of hydrogen bonds with asparagine, serine, tyrosine, and threonine residues in avidin providing stability to the complex. Furthermore, its valeric acid side chain can be derivatized in order to incorporate various reactive groups that facilitate the addition of a biotin tag to other molecules (Figure 18).

The streptavidin attachment to biotinylated surfaces provides both increased stability and organization of the streptavidin film at the surface. A study employing both surface plasmon resonance (SPR) and quartz crystal microbalance with energy dissipation monitoring (QCM-D) demonstrated that a streptavidin layer bound to a surface via biotin contained fewer trapped water molecules and was hence more compact than a streptaviding layer attached covalently to a surface, suggesting greater organization of the streptavidin surface bound via biotin.[56] In general, biotinylation is rapid, specific and unlikely to disturb the natural function of the molecule it attaches due to the small size of biotin (MW = 244.31 g/mol). Furthermore, biotin labelling is resistant to pH variations, high salt concentrations, heat extremes and denaturants, making the capture of biotinylated molecules possible in a wide variety of environments.

Determining the Attachment of Biotin to Thiol Groups

In this section, we shall investigate the attachment of biotin to thiolated Au-thin films. In particular we shall determine the biotin bonding to the thiol groups both in the absence of fluorescence as well as in the presence of fluorescent tagging.

AN INVESTIGATION OF NON-FLUORESCENT BIOTINYLATION

A widely used biotinylation reagent that is sulfhydryl reactive is biotin-maleimide (Figure 19). In particular maleimide reacts with reduced thiols groups attaching biotin to thiol containing molecules through *a stable thioether bond*.[57] The presence of PEG spacers increases the water solubility of the biotinylated molecule as well as suppressing the non-specific binding of target molecules to the surface.

The biotinylation of the surfaces can be accurately determined using characterization techniques such as infrared spectroscopy and X-ray photoelectron spectroscopy (XPS). In particular Booth et al.[58] synthesized biotinylated thiol, namely 11-mercaptododecanoic-(8-biotinoyl-amido-3,6-dioxaoctyl) amide) as seen in Figure 20 and then used it to form multilayer films on an Au surface.

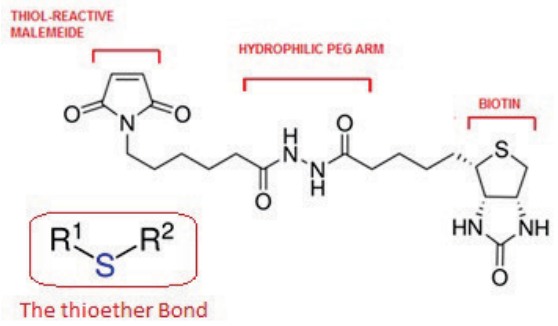

Figure 19. The biotin maleimide molecule incorporating a hydrophilic PEG arm and the thioether bond.

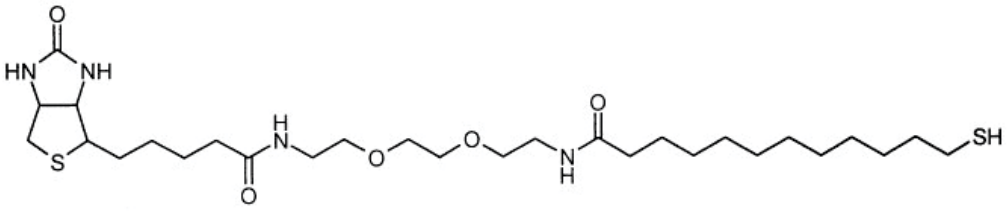

Figure 20. The biotin-thiol: (11-mercaptododecanoic-(8-biotinoyl-amido-3,6dioxaoctyl)amide).

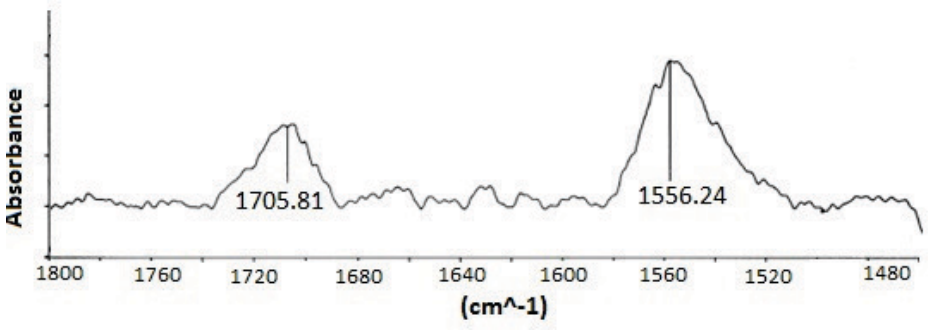

Figure 21. The IRAS spectrum of the biotin thiol on the Au-surface.[58]

In Figure 21 the IRAS spectrum of the film is depicted showing the biotin-thiol bond on an Au surface. In particular the peak at 1705.81 cm^{-1} corresponds to the amide vibration (amide I) of the urea group (predominantly the C=O stretching mode) while the peak at 1556.24 cm^{-1} corresponds to the amide II mode representing the out of phase combination of N-H in plane bending as well as C–N stretching vibrations.

Furthermore, XPS spectra are also recorded displaying an N-1s peak (Figure 22) both in the case of the biotin-thiol, but also of a biotinylation cholesterol derivate, namely 11-mercaptoundecanol. Additionally, a mixture of the two is investigated using XPS (N-1s peak).

In the case of the 11-mercaptoundecanol there is no signal corresponding to the N-1s peak in contrast to the biotin-thiol whose N-1s signal is the most prominent due to the nitrogen in the urea and amide groups of the molecule. We note that XPS showed further peaks corresponding to carbon, oxygen, carbon and sulfur in all cases.

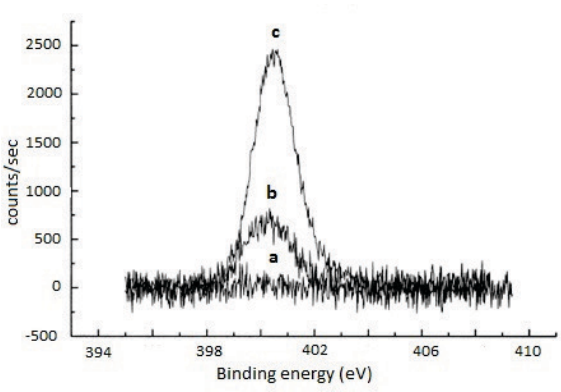

Figure 22. XPS spectra of the N-1s peak in the case of the following SAMs a. 100 % 11-mercaptoundecanol b. mixed (20 % biotin thiol and 80 % 11-mercaptoundecanol and c. 100 % biotin thiol as displayed in Figure 20.[58]

AN INVESTIGATION OF FLUORESCENT BIOTINYLATION

Fluorescence is a non-destructive way in life sciences for tracking and analyzing molecules. Apart from intrinsic fluorescence which is a natural property of some proteins and cell molecules, there is also extrinsic fluorescence where fluorophores, i.e. fluorescent dyes are used as labels for tracking and quantification purposes.[59] For example, the intensity of the emitted light from a fluorophore used to label a protein is proportional to the amount of the protein present. Furthermore, fluorophores have additional properties that can be utilized such as fluorescence resonance energy transfer (FRET, where the non-radiative energy transfer to a specific neighboring dye allows the detection of protein activation. Furthermore, property changes due to environmental conditions, e.g. intensity in certain dyes, make them appropriate for use in structural studies.[60]

Albeit the majority of works discuss the attachment of the fluorophore to the analyte, i.e target molecule, this can be at times either impossible or could lead to a risk of changing the interaction characteristics with affinity partners. Thus, a number of bioaffinity studies focus on the attachment of the fluorophore to the sensors surface functional group. In particular fluorescein-5 maleimide (Figure 23) can be used for this purpose, allowing both to quantitate available biotin binding sites, as well as the concentration of avidin or streptavidin due to the strong quenching effect when its molecule binds to avidin.

Ebner et al., showed the quantitation of biotin binding sites, using the biotin-4-fluorescein dye.[62] In particular, using fluorescence intensity and the concentration of biotin-binding protein the quantitation of available biotin binding sites was calculated. This was done for a specific amount of biotin-4 fluorescein, i.e. 8 nM, using the effect of fluorescence quenching upon binding to streptavidin (red), avidin (dark blue), streptavidin conjugates of the Alexa Fluor dye (orange) and alkaline phosphatase (light blue) as can be seen in Figure 24.

Fluorescently labeled biotins can also be used for the direct visualization of tagged proteins via fluorescence microscopy as can be seen in Figure 25. Using a light source of much higher intensity compared to the conventional

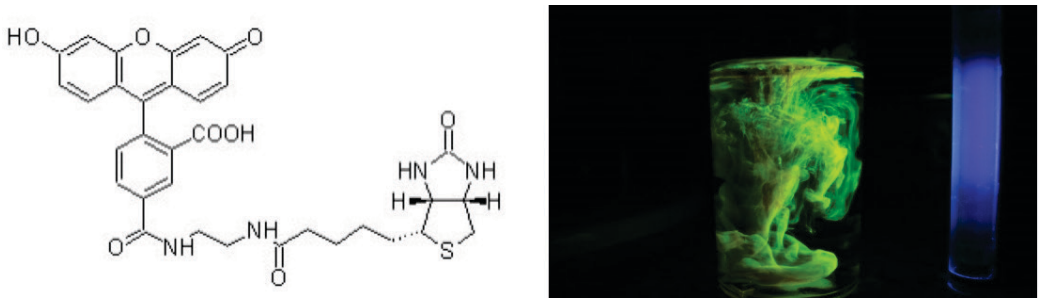

Figure 23. (a) Fluorescein-5 maleimide,[61] is a green fluorescent thiol-reactive dye (b) Fluorescein-5 maleimide under UV irradiation with peak excitation at 494 nm and peak emission at 521 nm.

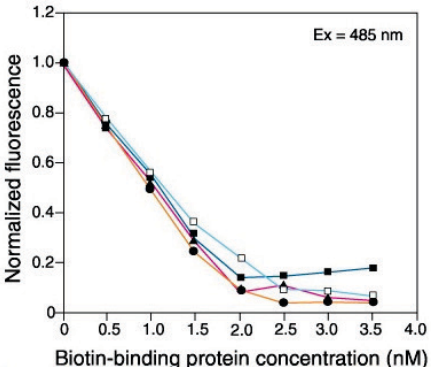

Figure 24. The quantitation of biotin-binding sites using 8 nM biotin-4-flurescein.[63]

light microscope, the fluorophores on the sample are excited. As a result, there is emission of longer wavelength light (lower energy) that leads to image magnification. It should be noted that the image obtained is not based on the light used to illuminate the sample, but rather from the emission wavelength of the fluorescent dye.

Furthermore fluorophore tagged biotin has been also studied within surface plasmon field enhance spectroscopy (SPFS). In particular SPFS excites the surface confined fluorophores using the enhanced electromagnetic field of the surface plasmon modes. In metal-dielectric interfaces, such as Au-water (buffer) we note that the surface plasmon evanescent field is enhanced by a factor of 16 leading to a strong fluorescence signal that accompanies binding events. SPFS in particular has shown promising results, leading to an enhanced signal compared to surface plasmon resonance by detecting binding to surfaces containing extremely diluted antigen density.[65,66]

Attaching Biotin to Silane Groups

Biotinylated molecules can also be immobilized on a silanized surfaces, such as silanized glass, ITO, or tin-doped indium oxide substrates for cell micropatterning and immunosensor development. In the area of optical biosensing, the attachment of biological probes to silica using silane coupling agents has been also successfully utilized in the Whispering Gallery Mode (WGM) optical

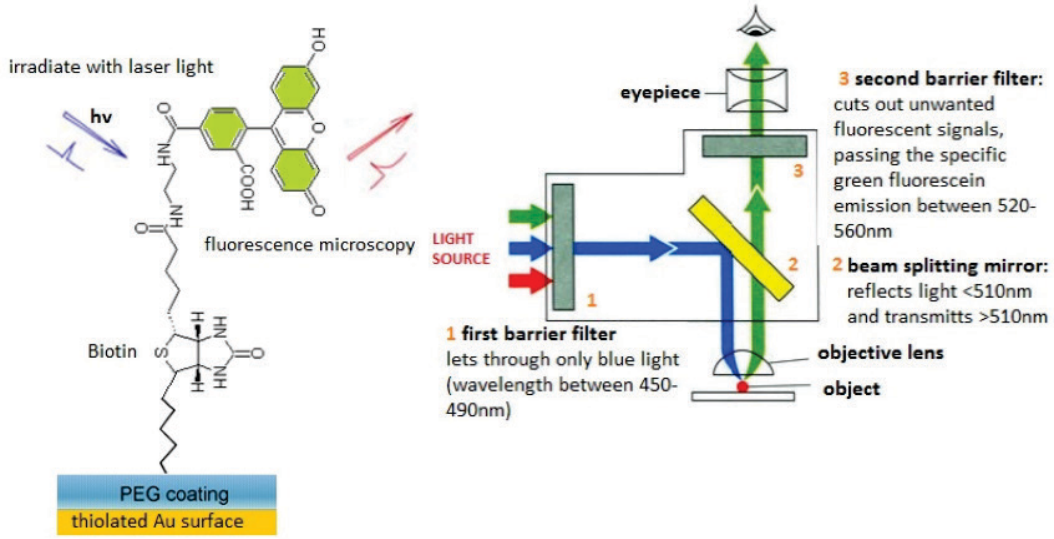

Figure 25. Fluorescence microscopy: the basic set up.[64]

microresonator biosensors. WGMs are a powerful tool for targeted detection of analytes at extremely low concentrations and although they can be fabricated in several geometries from a variety of material systems, the silica microsphere is the most common.[67,68] Silica surface chemistries may be applied to attach probe molecules to their surfaces. In particular, Soteropoulos et al.[69] used the avidin-biotin analyte-recognition element system, in conjunction with PEG non-fouling elements, in order to explore the extent of non-specific adsorption of lysozyme and fibrinogen at multiple concentrations, as well as the ability to detect avidin in a concentration-dependent fashion.

AN INVESTIGATION OF NON-FLUORESCENT BIOTINYLATION OF SILANE GROUPS

In general, a biotinylation reagent commonly used to modify surfaces such as glass or silica is the biotin carrying silane PEG (PEG-Si) (Figure 26) which is an ethoxyl or methoxyl silane functionalized polyethylene glycol. In particular it attaches to the SiO_2 film surfaces via a reaction between the hydroxyl groups and ethoxyl or methoxyl silane.

Lapin et al.[70] studied the biotinylation of silicon oxide surfaces using FTIR in order to provide direct information about the bonds formed during surface reactions. In particular, they functionalized silicon oxide surfaces using APTES (3-aminopropyltriethoxysilane) molecules which form covalent bonds to the surface forming a 3-aminopropylsiloxane (APS) film as seen in Figure 27. Finally, biotin-NHS (3-sulfo-N-hydroxysuccinimide ester sodium salt biotin) was bound covalently to the amine-terminated surface forming amide bonds.

In Figure 28. representative FTIR spectra is displayed for the biotinylation process of the APS surface which leads to covalent bonding (chemisorption).

We note that when the amine-terminated surface interacts with biotin-NHS a peak appears at 1540 cm^{-1} which is assigned to the N-H bend and C-N stretch of the amide II bands, while the peak at approximately 1660 cm^{-1} is assigned to the C=O stretch of the amide I vibrational modes, revealing the formation of an amide bond between biotin and the surface. Other bands at 1240 cm^{-1}, 1465 cm^{-1} and 1700 cm^{-1}, appear both in the chemisorbed and physisorbed biotin-NHS, suggesting they correspond to the alkyl chain and biotin fused rings of the biotin-NHS which are non-chemically reactive. In particular, the 1465 cm^{-1} peak corresponds to the CH_2 scissor mode of the alkyl chain which links the biotin fused rings to the NHS moiety, while the 1700 cm^{-1} peak describes the ureido carbonyl stretch mode of biotin-NHS. Furthermore, the 1240 cm^{-1} frequency band is associated with the biotin ureido group.

Chen et al.[71] also used a ToF-SIMS operating in the event-by-event bombardment/detection mode to characterize avidin-biotin assemblies on silane-modified glass substrates. SIMS was used to analyze several variants of the biointerface, including avidin physically adsorbed on a monofunctional acryl silane surface and covalently attached on a mono-functional (amine terminated) and a bi-functional (amine and acryl terminated) silanes. The goal of these studies was to determine the density of avidin and biotin layers chemical or physically adsorbed on silanized glass substrate.[72] Other approaches that have been used in literature include ellipsometry, contact angle measurement, fluorescence microscopy, and optical resonator characterization methods to study non-specific adsorption, the quality of the functionalized surface and the biosensor's performance.

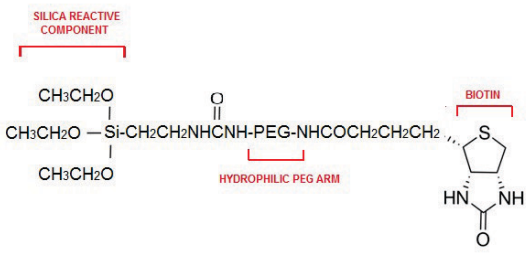

Figure 26. The biotin carrying silane PEG (PEG-Si).

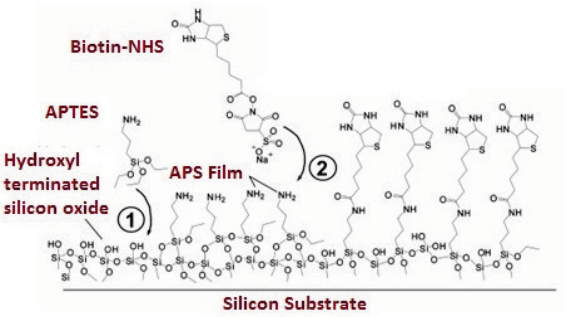

Figure 27. Attaching biomolecules to silicon oxide surface.[70]

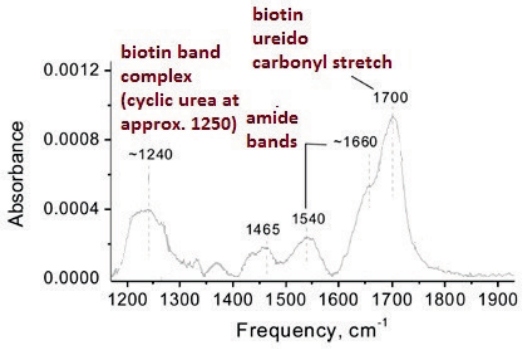

Figure 28. FTIR spectra of an APS biotinylated (Biotin-NHS) surface using chemisorption.[70]

A FLUORESCENT BIOTINYLATION OF SILANE GROUPS

Fluorescent biotin conjugates can be used in a similar manner for the quantitation of available biotin-binding sites as well as the concentration of Avidin or Streptavidin upon binding. For this purpose, fluorescein isothiocyanate (FITC) can be attached to biotin carrying silanes, such as A-AM silane (N-2 (aminoethyl)-3-aminopropyltrimethoxy-silane) or B-AM silane (N-phenyl-3-aminopropyltrimeth-oxysilane). In particular FITC is obtained by the funct-ionalization of the fluorescein molecule by an isothio-cyanate reactive group (–N=C=S) as seen in Figure 29. The imaging of fluorophore tagged biotin on silanized surfaces can be done using fluorescent microscopy and surface plasmon field enhanced spectroscopy (SPFS) following the same principles that were described in the characterization of fluorophore tagged biotin on thiolated surfaces.

In another study, Isoda et al.,[73] presented a method to prevent denaturation of biopolymers, by trapping a polynucleotide on a substrate by hydrogen bonding using silica particles with surfaces modified by aminoalkyl chains. The amino groups introduced on the surface can interact with single-stranded nucleic acids through hydrogen bonding, resulting in a conjugate between a polynucleotide and inorganic material. After, preparation the functional groups on the surface of the aminoalkylated SiO_2 particles were qualitatively analyzed by Fourier transform infrared. The substitution of aminoalkyl chains on the SiO_2 surface was further confirmed by fluorescence labeling using FITC. The single-stranded nucleic acid trapped to the silica particle was further interacted by an acridine orange derivative as a fluorescent label, allowing changes in fluorescence intensity originating from interactions between the single-stranded nucleic acid and aromatic compounds to be investigated.

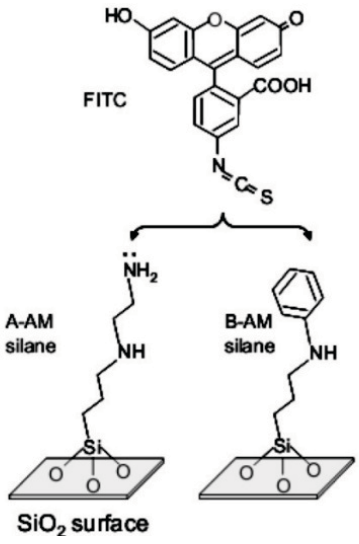

Figure 29. Silane fluorescence labeling using FITC.[73]

CONCLUSIONS

Surface modification techniques focusing on Au thiolation and salinization of SiO_2 surfaces were presented in this paper, with a focus on creating primarily platforms in the fabrication of biosensors. Both types of thiols and silanes are shown to be strong surface anchors providing stability to SAMs which is critical to withstanding subsequent processing and measurement conditions. In general, there is a lot of scope in SAMs towards providing better surface passivation, prevent oxidation, aid or prevent wetting and help with reducing the denaturation of biomolecules on biosensors surfaces as well as increasing the lifetime and efficiency of biosensing systems. Additionally, subsequent surface biotinylation was reviewed as an important tool for attaching a variety of molecules to surfaces, via the strong affinity association constant of 10^{15} M^{-1} with avidin, allowing for countless applications within life sciences. In general, the performance of the biosensor is highly dependent on the substrate material used and its careful modification and verification proper adhesion of the SAM monolayer as well as further successful biotinylation. In this regard, predominantly spectroscopic and microscopic techn-iques are commonly employed for characterization purposes.

REFERENCES

[1] D. Prashar, *Int. J. Chemtech Res.* **2012**, *4*(*1*), 258–265.
[2] N. K. Chaki, K. Vijayamohanan, *Biosens. Bioelectron.* **2002**, *17*, 1–12. https://doi.org/10.1016/S0956-5663(01)00277-9
[3] S. Karapetis, T. Hianik, D. Nikolelis, *Sensors* **2018**, *18*(*12*), 4218. https://doi.org/10.3390/s18124218
[4] R. Colorado, T. R. Lee, *Encyclopedia of Materials: Science and Technology*, **2001**, 9332–9344. https://doi.org/10.1016/B0-08-043152-6/01682-X
[5] S. Creager, *Encyclopedia of Materials: Science and Technology*. **2001**, pp. 8299–8304. https://doi.org/10.1016/B0-08-043152-6/01485-6
[6] C. Nicosia, J. Huskens, *Mater. Horiz*. **2014**, 1, 32–45. ttps://doi.org/10.1039/C3MH00046J
[7] O. Seitz, P. G. Fernandes, R. Tian, N. Karnik, H. C. Wen, H. Stiegler, R. A. Chapman, E. M. Vogel, Y. J. Chabal, *J. Mater. Chem.* **2011***, 21*, 4384–4392. https://doi.org/10.1039/c1jm10132c
[8] A. Singh, I. S. Lee, K. Kim, A. S. Myerson, *Cryst. Eng. Comm.* **2011**, *13*, 24–32. https://doi.org/10.1039/C0CE00030B
[9] J. Noh, M. Hara, *Langmuir* **2001**, *17*(*23*), 7280–7285. https://doi.org/10.1021/la0100441
[10] D. K. Schwartz, Annu. Rev. Phys. Chem. **2001**, *52*(*1*), 107–137. https://doi.org/10.1146/annurev.physchem.52.1.107

[11] J. G. Vos, R. J. Forster, T. E. Keyes in *Interfacial Supramolecular Assemblies*, John Wiley & Sons **2003**, pp. 88–94. https://doi.org/10.1002/0470861517

[12] N. K Chaki, M Aslam, J. Sharma, K Vijayamohanan, *Proc. Indian Acad. Sci. (Chem. Sci.)* **2001**, *113*, 659–670. https://doi.org/10.1007/BF02708798

[13] A. Laromaine, C. R. Mace in *Organic Nanomaterials: Synthesis, Characterization, and Device Applications*, (Eds.:T. Torres, G. Bottari), John Wiley & Sons, **2013**, pp. 369–395. https://doi.org/10.1002/9781118354377.ch17

[14] S.Patai, *The chemistry of the thiol group*. London: Wiley, **1974**.

[15] S. Karapetis, T. Hianik, D. Nikolelis, *Sensors* **2018**, *18* (*12*), 4218. https://doi.org/10.3390/s18124218

[16] E. Reimhult, F. Höök, *Sensors* **2015**, *15*, 1635–1675. https://doi.org/10.3390/s150101635

[17] C. J. Love, L. A. Estroff, J. K. Kriebel, R. G. Nuzzo, G. M. Whitesides, *Chem. Rev*. **2005**, *105*(*4*), 1103–1170. https://doi.org/10.1021/cr0300789

[18] M. Boeckl, D. Graham, *Mater. Matters* **2006***, 1.2,* 3.

[19] D. M. Alloway, A. L. Graham, X. Yang, A. Mudalige, R. Colorado, V. H. Wysocki, J. E. Pemberton, T. Randall, R. J. Wysocki, N. R. Armstrong, *J. Phys. Chem C* **2009**, *113*(*47*), 20328–20334. https://doi.org/10.1021/jp909494r

[20] S.-W. Tam-Chang, I. Iverson, Studies in Surface Science and Catalysis, **1999**, *120*, 917–950. https://doi.org/10.1016/S0167-2991(99)80576-X

[21] *Silane and Other Coupling Agents*, Vol. 2, (Ed.: K. L. Mittal), VSP, The Netherlands, **2000**.

[22] SiSiB Silanes, **1999**. http://www.powerchemical.net/coupling1.htm [Accessed 25th August, 2020]

[23] C. Kim, A. R. Jang, D. J. Kang, *Curr. Appl. Phys.* **2009**, *9*(*6*), 1454–1458. https://doi.org/10.1016/j.cap.2009.03.023

[24] C. Hayichelaeh, L. A. E. M. Reuvekamp, W. K. Dierkes, A. Blume, J. W. M. Noordermeer, K. Sahakaro, *Polymers* **2018**, *10*(*6*), 584. https://doi.org/10.3390/polym10060584

[25] B. Bharat, K. J. Kwak, S. Gupta, S. C. Lee, *J. R. Soc. Interface* **2009**, *6*(*37*), 719–733. https://doi.org/10.1098/rsif.2008.0398

[26] T. Janči, L. Mikac, M. Ivanda, N. Marušić Radovčić, H. Medić, S. Vidaček, *J. Raman Spectrosc.* **2017**, *48*(*1*), 64–72. https://doi.org/10.1002/jrs.4991

[27] M. Kosović, M. Balarin, M. Ivanda M, et al., *Appl Spectrosc*. **2015**, *69*(*12*), 1417–1424. https://doi.org/10.1366/14-07729

[28] L. Mikac, M. Ivanda, M. Gotić, T. Mihelj, L. Horvat, *J. Nanopart. Res.* **2014**, 16, 2748. https://doi.org/10.1007/s11051-014-2748-9

[29] L. G. Bousiakou, H. Gebavi, L. Mikac et al., *Croat. Chem. Acta* **2019**, 92(4). 479–494. https://doi.org/10.5562/cca3558

[30] S. Fearn, An Introduction to Time-of-Flight Secondary Ion Mass Spectrometry (ToF-SIMS) and its Application to Materials Science, IOP Publishing, UK, **2015**. https://doi.org/10.1088/978-1-6817-4088-1ch5

[31] S. Aoyagia, A. Rouleau, W. Boireau, *Appl. Surf. Sci*. **2010**, *255*, 1071–1074. https://doi.org/10.1088/978-1-6817-4088-1ch5

[32] P. K. Sarswat, A. Sathyapalan, M. L. Free, *Anti-Abrasive Nanocoatings,* Elsevier, **2015**, 331–348. https://doi.org/10.1016/B978-0-85709-211-3.00013-3

[33] H. Hamoudi, M. Prato, C. Dablemont, O. Cavalleri, M. Canepa, V. A. Esaulov, *Langmuir* **2010**, *26*(*10*), 7242–7247. https://doi.org/10.1021/la904317b

[34] H. Hamoudi, Z. Guo, M. Prato, C. Dablemont, W. Q. Zheng, B. Bourguignon, M. Canepad, V. A. Esaulov, *Phys. Chem. Chem. Phys.* **2008**, *10*, 6836–6841. https://doi.org/10.1039/b809760g

[35] R. K. Smith, P. A. Lewis, P. S. Weiss, *Prog. Surf. Sci.* **2004**, *75*, 1–68. https://doi.org/10.1016/j.progsurf.2003.12.001

[36] H. C. Kwon, A. A. Gewirth, *J. Phys. Chem. B* **2005**, *109*(*20*), 10213–10222. https://doi.org/10.1021/jp044655o

[37] K. C. Langry, T. V. Ratto, R. E. Rudd, M. W. McElfresh, *Langmuir* **2005**, *21*(*26*), 12064–12067. https://doi.org/10.1021/jp044655o

[38] G. H. Cross, A. A. Reeves, S. Brand, J. F. Popplewell, L. L. Peel, M. J. Swann, N. J. Freeman, *Biosens. Bioelectron.* **2003**, *19*(*4*), 383–390. https://doi.org/10.1016/S0956-5663(03)00203-3

[39] M. J. Swann, N. J. Freeman, G. H. Cross in *Handbook of Biosensors and Biochips* (Eds.: R. S. Marks, C. R. Lowe, D. C. Cullen, H. H. Weewall, I. Karube), John Wiley & Sons, **2007**, pp. 549–568.

[40] L. S. Alarcón, L. Chen,V. A. Esaulov, J. E. Gayone, E. A. Sánchez, O. Grizzi, *J. Phys. Chem. C* **2010**, *114*(*47*), 19993–19999. https://doi.org/10.1021/jp1044157

[41] R. L. Garrell, C. Szafranski, W. Tanner, Surface Enhanced Raman Spectroscopy of Thiols and Disulfides, Raman and Luminescence Spectroscopies in Technology, SPIE 1336, **1990**, 11, 264–271 https://doi.org/10.1117/12.22917

[42] C A. Szafranski, W Tanner, P E. Laibinis, R L. Garrell, *Langmuir* **1998**, *14*(*13*), 3570–3579. https://doi.org/10.1117/12.22917

[43] D. A. Stern, E. Wellner, G. N. Salaita, L. Laguren-Davidson, F. Lu, N. Batina, D. G. Frank, D. C. Zapien, N. Walton, A. T. Hubbard, *J. Am. Chem. Soc.* **1988**, *110*, 4885–4893. https://doi.org/10.1021/la9702502

[44] F. J. Himpsel, Chapter: Ultraviolet Photoelectron Spectroscopy in Characterization of Materials, 2nd edition, Wiley, **2012**. https://doi.org/10.1002/0471266965.com061.pub2

[45] D. G. Castner, K. Hinds, D. W. Grainger, *Langmuir* **1996**, *12*(*21*), 5083–5086 https://doi.org/10.1021/la960465w

[46] D. M. Alloway, M. Hofmann, D. L. Smith, N. E. Gruhn, A. L. Graham, R. Colorado, V. H. Wysocki, T. R. Lee, P. A. Lee, N. R. Armstrong, *J. Phys. Chem. B* **2003**, *107*(*42*), 11690–11699. https://doi.org/10.1021/jp034665+

[47] D. M. Rousseau et al., *J. Phys. Chem. B* **2006**, *110*(*22*), 10862–10872. https://doi.org/10.1021/jp061720g

[48] L. B. Capeletti, J. H. Zimnoch in Applications of Molecular Spectroscopy to Current Research in the Chemical and Biological Sciences (Ed.: M. Stauffer), IntechOpen, **2016**, pp. 3–22.

[49] C. L. Cherkouk, L. Rebohle, W. Skorupa, T. Strache, H. Reuther, M. Helm, *J Colloid Interface Sci.* **2009**, *337*(*2*), 375–380. https://doi.org/10.1016/j.jcis.2009.05.045

[50] G. Jakša, B. Štefane, J. Kovač, *Surf. Interface Anal.* **2013**, *45*, 1709–1713 https://doi.org/10.1002/sia.5311

[51] L. Haeussliny, H. Ringsdorf, F. J. Schmitt, W. Knoll, *Langmuir* **1991**, *7*(*9*), 1837–1840. https://doi.org/10.1021/la00057a001

[52] J. Anzai, T. Hoshi, T. Osa, *Avidin—Biotin Mediated Biosensors* in *Biosensors and Their Applications* (Eds.: V. C. Yang, T. T. Ngo), Springer, Boston, MA, **2000**. https://doi.org/10.1007/978-1-4615-4181-3_3

[53] R. Conners, E. Hooley, A. R. Clarke, S. Thomas, R. L. Brady, *J. Mol. Biology* **2006**, *357*(*1*), 263–274. https://doi.org/10.1016/j.jmb.2005.12.054

[54] O. Livnah, E. A. Bayer, M. Wilchek, J. L. Sussman, PNAS USA **1993**, *90*, 5076–5080. https://doi.org/10.1073/pnas.90.11.5076

[55] Thermo Scientific EZ-Link Biotinylation Reagents, Thermo Scientific Avidin-Biotin Technical Handbook, **2009** Thermo Fisher Scientific Inc, US.

[56] N. A. Lapin, Y. J. Chabal. *J Phys. Chem. B*. **2009**, *113*(*25*), 8776–8783. https://doi.org/10.1021/jp809096m

[57] Easy molecular bonding crosslinking technology Reactivity chemistries, applications and structure references, Thermo Scientific Crosslinking Technical Handbook **2012** Thermo Fisher Scientific Inc, US

[58] C. Booth, R. J. Bushby, Y. Cheng, S. D Evans, Q. Liu, H. Zhang, *Tetrahedron*. **2001**, *57*(*49*), 9859–9866. https://doi.org/10.1016/S0040-4020(01)01003-1

[59] V. P. Hytönen, *Cell Chem. Biol.* **2017**, *24*(*8*), 921–922. https://doi.org/10.1016/j.chembiol.2017.07.013

[60] K. Nishi, S. I. Isobe, Y. Zhu, R. Kiyama, *Sensors* **2015**, *15*(*10*), 25831–25867. https://doi.org/10.3390/s151025831

[61] Fluorescein-5-maleimide, **2015**. https://biotium.com/product/fluorescein-5-maleimide [Accessed 25th August, 2020]

[62] A. Ebner, M. Marek, K. Kaiser, G. Kada, C. D. Hahn, B. Lackner, H. J. Gruber, *Methods Mol. Biol.* **2008**, *418*, 73–88. https://doi.org/10.1007/978-1-59745-579-4_7

[63] F. Yu, D. Yao, W. Knoll, *Analytical Chemistry* **2003**, *75*(*11*), 2610–2617. https://doi.org/10.1021/ac026161y

[64] M. J. Sanderson, I. Smith, I. Parker, M. D. Bootman, *Cold Spring Harb. Protoc.* **2014**, *10*, 1042–1065. https://doi.org/10.1101/pdb.top071795

[65] W. Knoll, *Annu. Rev. Phys. Chem.* **1998**, *49*, 569–638. https://doi.org/10.1146/annurev.physchem.49.1.569

[66] R. J. Green, R. A. Frazier, K. M. Shakesheff, M. C. Davies, C. J. Roberts, S. J. Tendler, *Biomaterials* **2000**, *21*, 1823–1835. https://doi.org/10.1016/S0142-9612(00)00077-6

[67] D. Ristić, A. Chiappini, M. Mazzola, D. Farnesi, G. Nunzi-Conti, G. Righini, P. Féron, G. Cibiel, M. Ferrari, M. Ivanda, *The European physical journal, Special topics* **2014**, *223*(*10*), 1959–1969. https://doi.org/10.1140/epjst/e2014-02239-2

[68] L. J. Chen, J. H. Seo, M. J. Eller et al. *Anal Chem*. **2011**, *83*(*18*), 7173–7178. https://doi.org/10.1021/ac2016085

[69] C. E. Soteropulos, H. K. Hunt, *J. Vis. Exp.* **2012**, *63*, e3866. https://doi.org/10.3791/3866

[70] N. A. Lapin, Y. J. Chabal, *J. Phys. Chem. B* **2009**, *113*(*25*), 8776–8783. https://doi.org/10.1021/jp809096m

[71] L. J. Chen, J. H. Seo, M. J. Eller et al., *Anal Chem*. **2011**, *83*(*18*), 7173–7178. https://doi.org/10.1021/ac2016085

[72] F. Wang, M. Anderson, M. T. Bernards, H. K. Hunt. *Sensors*. **2015**, *15*(*8*), 18040–18060. https://doi.org/10.3390/s150818040

[73] T. Isoda, R. Maeda, *J. Funct. Biometer.* **2012**, *3*(*3*), 601–614. https://doi.org/10.3390/jfb3030601